Synaptobrevin-2 dependent regulation of single synaptic vesicle endocytosis

Natali L. Chanaday[a],* and Ege T. Kavalali[a,b],*
[a]Department of Pharmacology, School of Medicine and [b]Vanderbilt Brain Institute, Vanderbilt University, Nashville, TN 37240-7933

ABSTRACT Evidence from multiple systems indicates that vesicle SNARE (soluble NSF attachment receptor) proteins are involved in synaptic vesicle endocytosis, although their exact action at the level of single vesicles is unknown. Here we interrogate the role of the main synaptic vesicle SNARE mediating fusion, synaptobrevin-2 (also called VAMP2), in modulation of single synaptic vesicle retrieval. We report that in the absence of synaptobrevin-2, fast and slow modes of single synaptic vesicle retrieval are impaired, indicating a role of the SNARE machinery in coupling exocytosis to endocytosis of single synaptic vesicles. Ultrafast endocytosis was impervious to changes in the levels of synaptobrevin-2, pointing to a separate molecular mechanism underlying this type of recycling. Taken together with earlier studies suggesting a role of synaptobrevin-2 in endocytosis, these results indicate that the machinery for fast synchronous release couples fusion to retrieval and regulates the kinetics of endocytosis in a Ca^{2+}-dependent manner.

INTRODUCTION

In central synapses, synaptobrevin2 (syb2, also called VAMP2) is the predominant synaptic vesicle SNARE protein that interacts with the plasma membrane SNAREs SNAP-25 and syntaxin1 to execute exocytosis (Südhof and Rothman, 2009). Several lines of evidence suggest key functions for the SNARE complex in the regulation of vesicle recycling and thus in the coupling of fusion and endocytosis (Deak et al., 2004; Xu et al., 2013). The involvement of syb2 in endocytic trafficking could be of two types. First, it may be involved in fusion pore regulation (Wu et al., 2017; Bao et al., 2018; Chiang et al., 2018). Second, syb2 may be involved in tagging synaptic vesicles for rapid retrieval independently of its SNARE function. Earlier work from our laboratory suggested a role for syb2 in rapid coupling of vesicle fusion and retrieval during neuronal activity. Loss of syb2 altered the kinetics of FM dye release and also impaired endo-

cytosis that is tightly coupled to exocytosis (Deak et al., 2004). Subsequent work conducted in multiple preparations validated these initial findings (Hosoi et al., 2009; Xu et al., 2013, Koo et al., 2015). While these earlier studies have focused on aggregate retrieval of multiple vesicles following strong stimulation, they have not defined a precise role of syb2 in endocytosis of single synaptic vesicles. Therefore, here we investigated the role of syb2 in endocytosis of single synaptic vesicle by visualizing retrieval events in syb2-deficient synapses. We found that, although loss of syb2 slowed down retrieval after strong stimulation, suggesting that syb2 may accelerate endocytosis during high-frequency firing, syb2 acts to delay retrieval of individual synaptic vesicles fused after a single action potential (AP), a behavior that resembles that of its partner synaptotagmin-1 (syt1). These findings strongly support a role for the fusion machinery in coupling different modes of neurotransmitter release to separate pathways of synaptic vesicle recycling.

RESULTS AND DISCUSSION

Synaptobrevin-2 regulates exo-endocytosis coupling after high-frequency stimulation

To optically monitor synaptic vesicle trafficking we used the vesicular glutamate transporter 1 (vGluT1) fused to the pH-sensitive GFP (pHluorin) in one of its luminal loops (Voglmaier et al., 2006). This probe possesses the major advantages of having a better signal-to-noise ratio compared with other synaptic vesicle probes and of presenting a highly selective localization to synaptic vesicles compared
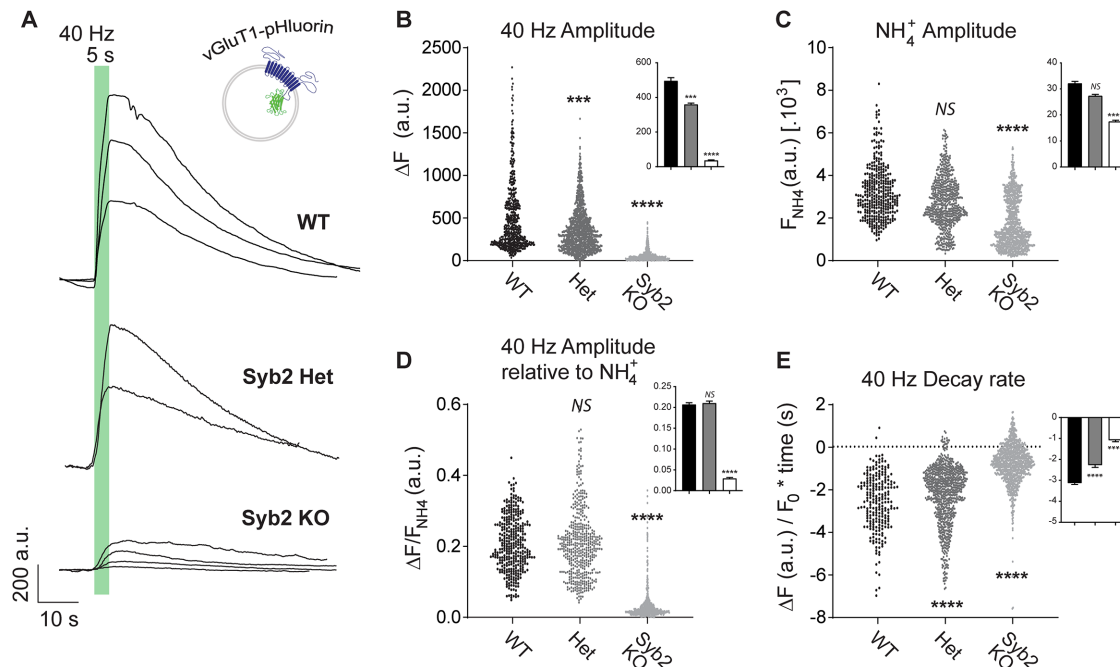
FIGURE 1: Synaptic vesicle fusion and endocytosis after high-frequency stimulation are impaired in the absence of syb2. (A) Example traces of vGluT1-pHluorin fluorescence in response to high-frequency stimulation (40 Hz, 5 s) in syb2 KO neurons, syb2 heterozygous, and littermate control (WT). (B) Amplitude (ΔF) of vGluT1-pHluorin peak for control (WT), syb2 heterozygous (Het), and syb2 KO neurons. Kruskall-Wallis test: $p < 0.0001$. Dunn's multiple comparison's test: WT vs. Het, ***, $p = 0.0010$; WT vs. syb2 KO, ****, $p < 0.0001$. Inset: average values $\pm$ SEM. (C) Maximal vGluT1-pHluorin fluorescence measured with 50 mM NH_4^+ perfusion. Kruskall-Wallis test: $p < 0.0001$. Dunn's multiple comparison's test: WT vs. Het, NS, $p = 0.0932$; WT vs. syb2 KO, ****, $p < 0.0001$. Inset: average values $\pm$ SEM. (D) Amplitude of vGluT1-pHluorin peak normalized to maximal possible fluorescence (50 mM NH_4^+). Kruskall-Wallis test: $p < 0.0001$. Dunn's multiple comparison's test: WT vs. Het. NS; $p > 0.9999$; WT vs. syb2 KO. ****, $p < 0.0001$. Inset: average values $\pm$ SEM. (E) Rate of vGluT1-pHluorin fluorescence decay (calculated by linear fitting of the 95–50% range of the peak decay region). Kruskall-Wallis test: $p < 0.0001$. Dunn's multiple comparison's test: WT vs. Het, ****, $p < 0.0001$; WT vs. syb2 KO, ****, $p < 0.0001$. Inset: average values $\pm$ SEM. For all figures, at extracellular 2 mM Ca^{2+}: control (WT): three E17–19 pups from three litters, $N = 570$ boutons (six coverslips). Het: six E17–19 pups from five litters, $N = 1190$ boutons (12 coverslips). Syb2 KO: six E17–19 pups from five litters, 1295 boutons (18 coverslips). For all figures, at extracellular 8 mM Ca^{2+}: control (WT): $N = 340$ boutons (four coverslips). Het: $N = 910$ boutons (11 coverslips). Syb2 KO: 1062 boutons (17 coverslips).

with other membranous compartments (Leitz and Kavalali, 2011; Kavalali and Jorgensen, 2014). VGluT1-pHluorin fluorescence is quenched at the acidic luminal pH of synaptic vesicles, but upon fusion vGluT1-pHluorin gets exposed to the extracellular pH and fluorescence increases (Figure 1A). After a short period of high-frequency stimulation (40 Hz, 5 s), which mobilizes numerous vesicles of the recycling pool, we observed a marked reduction in release in synapses lacking syb2 (Syb2 knock-out –KO–), revealed as an ~90% decrease in the peak amplitude of vGluT1-pHluorin (Figure 1, A and B). Moreover, >99.5% of synapses responded to the high-frequency stimulation in wild-type (WT) and syb2 heterozygous synapses, while only 12–30% of synapses were active in these conditions in different syb KO cultures. There was an apparent gene dose effect on fusion, because heterozygous neurons (50% syb2 gene dose; Het) mobilized ~30% less vGluT1-pHluorin than WT littermate controls (Figure 1B). To measure the size of the total synaptic vesicle pool, a 50 mM NH_4Cl solution was perfused to render acidic organelles alkaline and reveal the maximal pHluorin signal (Figure 1C). This treatment showed a trend to a syb2 gene dose–dependent reduction in the total synaptic vesicle pool, consistent with a role for syb2 in vesicle biogenesis and/or maintenance (Figure 1C). However, our laboratory previously quantified synaptic vesicle numbers in syb2 KO hippocampal synapses by electron microscopy and

found no differences between syb2 KO and littermate WT synapses (Deak et al., 2004). The present finding, then, may indicate that other factors rather than synaptic vesicle biogenesis might be altered in syb2 KO neurons, including potential alterations in vesicle acidification (Haberman et al., 2012) or protein recruitment to synaptic vesicles (including vGluT1-pHluorin). In agreement with this notion, when normalized to NH_4Cl response, the amplitude of vGluT1-pHluorin response to high-frequency stimulation was similar for WT and Het, but significantly decreased for syb2 KO (~85% reduction; Figure 1D). This result suggests that a mere reduction in syb2 protein levels may not affect synaptic vesicle fusion but may alter the fraction of vesicles that are mobilized. Syb2 is a highly abundant presynaptic protein per vesicle believed to be in excess of the numbers required for function (Takamori et al., 2006); accordingly, our results support the notion that to reveal syb2's role in synaptic vesicle endocytosis a complete deletion of the protein is necessary.

After the stimulation period, the time course of endocytosis is related to the kinetics of decay in vGluT1-pHluorin fluorescence (Figure 1A). This decrease in fluorescence results from a combination of retrieval from the plasma membrane of the fused synaptic vesicle proteins and reacidification of the endosomal intermediates generated. In presynaptic terminals lacking syb2, fusion of synaptic
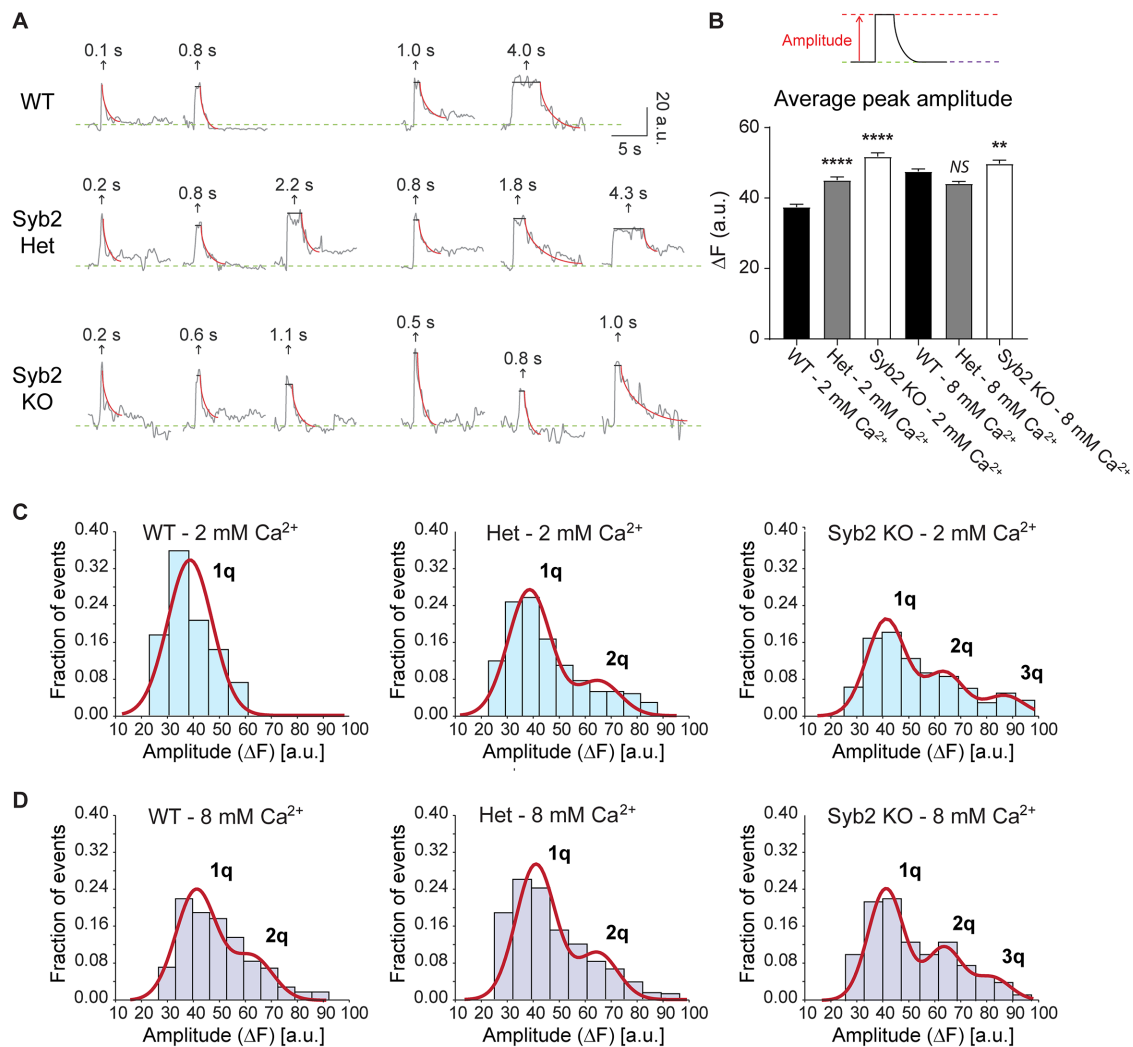
FIGURE 2: Deleting syb2 increases the amplitude of single synaptic vesicle fusion events measured with vGluT1-pHluorin. (A) Example fluorescence traces of vGluT1-pHluorin single synaptic vesicle fusion events detected during sparse stimulation (0.1–0.05 Hz, 20–25 APs). (B) Average fluorescence amplitude (ΔF) of single synaptic vesicle fusion events. Kruskall-Wallis test: $p < 0.0001$. Dunn's multiple comparison's test for 2 mM Ca^{2+}: WT vs. Het, $p < 0.0001$; WT vs. syb2 KO, $p < 0.0001$. Dunn's multiple comparison's test for 8 mM Ca^{2+}: WT vs. Het, $p = 0.0754$; WT vs. syb2 KO, $p < 0.0001$. WT 2 mM Ca^{2+} vs. WT 8 mM Ca^{2+}, $p < 0.0001$. (C, D) Probability distributions of single synaptic vesicle amplitudes (bars) with a Gaussian mix model fit (straight red lines).

vesicles is followed by a slow and constant decay in fluorescence in contrast to the classical faster and exponential decay in littermate WT controls (Figure 1E). Thus, the rate of decay during the first 10 s poststimulation were calculated and compared among groups to reduce fitting errors (Figure 1E). This slowdown in the kinetics of endocytosis in syb2 KO synapses is gene dose dependent (Figure 1E) and it points to a role of syb2 and possibly the canonical SNARE machinery in modulating synaptic vesicle retrieval. These results bolster the earlier findings that syb2 couples fusion to endocytosis after high-frequency stimulation. In the absence of syb2, retrieval after strong stimulation may be decoupled from release leading to a slowdown in the progression of endocytosis, which may partly be due to the dominant function of other vesicular SNAREs. One candidate is VAMP4, which was previously shown to partially rescue syb2 KO and targets vesicles to a slower retrieval pathway (Raingo et al., 2012). Synaptobrevin-1 is another SNARE that was proposed to mediate compensatory endocytosis in a fraction of autaptic synapses lacking syb2 (Zimmermann et al., 2014), although our group

did not find detectable levels of synaptobrevin-1 or cellubrevin (VAMP3) in hippocampal dissociated cultures (Schoch et al., 2001).

Synaptobrevin-2 couples fusion of single synaptic vesicles to a fast mode of retrieval

We next analyzed single synaptic vesicle fusion events in syb2 KO neurons using low-frequency stimulation (0.1–0.05 Hz, 20–25 APs) and our previously described method (Chanaday and Kavalali, 2018). Despite the lower release probability caused by elimination of syb2, fusion events were detectable (Figure 2A). The amplitude of these single synaptic vesicle release events depends on the number of vGluT1-pHluorin molecules per vesicle and the number of vesicles fused (i.e., multivesicular release). When we analyzed the amplitudes in syb2 KO synapses and compared with littermate WT and heterozygous neurons, we observed a significant ~20% increase in the average amplitude (Figure 2B) due to the appearance of events with larger amplitudes in the absence of syb2 (Figure 2C). In WT hippocampal synapses, rising extracellular Ca^{2+} concentration not

only increases release probability but also causes multivesicular release, due to near simultaneous fusion of more than one vesicle per presynaptic bouton (Leitz and Kavalali, 2011; Chanaday and Kavalali, 2018). This phenomenon can be observed as the emergence of multiquantal peaks when the amplitude distribution is fitted with a Gaussian mix (compare 2 and 8 mM Ca^{2+} in Figure 2, C and D; also see Leitz and Kavalali, 2011). In neurons lacking syb2, quantal events (corresponding to one synaptic vesicle) are reduced and multiquantal fusion events are increased compared with WT (Figure 2, C and D). Given the nature of the technique, we cannot discriminate whether this observation results from a higher incidence of multivesicular release at syb2 KO presynaptic terminals or from larger vesicles containing additional copies of vGluT1-pHluorin. The latter hypothesis is consistent with a previous report from our group which detected an increase in synaptic vesicle size in syb2 KO synapses (Deak *et al.*, 2004; also see Imig *et al.*, 2014). Moreover, in *Drosophila* photoreceptors, elimination of syb2 leads to presynaptic endolysosomal trafficking defects that leads to accumulation of membranous compartments (Haberman *et al.*, 2012). Such deficits may explain the presence of larger vesicles with, possibly, a higher copy number of vGluT1-pHluorin. In an earlier study (Deak *et al.*, 2004), we had reported a 30% increase in vesicle diameter that would lead to increases of ~70% in surface area and ~100% in vesicle volume, and as such may explain the origin of the multiquantal (2q and 3q) peaks in the distribution (Figure 2, C and D).

Visualization of single vesicle fusion events using vGlut-pHluorin enables analytical separation of fusion from retrieval and reacidification processes (Leitz and Kavalali, 2016). After fusion, fluorescence remains relatively constant as long as clusters of vGluT1-pHluorins remain in contact with the extracellular space within the region of interest (dwell time). When the probes are endocytosed and reacidification starts, fluorescence decays back to baseline. Thus, the dwell time reports the kinetics of retrieval while the fluorescence decay is indicative of the kinetics of reacidification (Leitz and Kavalali, 2011; Chanaday and Kavalali, 2018). Here, we applied our previously described analysis of dwell times (Chanaday and Kavalali, 2018).

Using this improved analysis, we corroborated our previous finding that multiple pathways with distinct kinetics coexist at presynaptic terminals (Figure 3A). Ultrafast (<400–500 ms), fast (~1–1.5 s), and slow (3–5 s) modes of synaptic vesicle protein retrieval are present at WT and syb2 Het (50% gene dose) presynaptic boutons (Figure 3C). As shown before (Leitz and Kavalali, 2011; Chanaday and Kavalali, 2018), increasing extracellular Ca^{2+} concentration from 2 to 8 mM produces a slowdown in endocytosis detected as prolongation of dwell times (Figure 3B). In particular, we observed a Ca^{2+}-dependent deceleration of the slow component of retrieval. When syb2 levels are reduced, the slow (3–5 s) pathway of synaptic vesicle retrieval is greatly reduced (60% reduction in the proportion of slow events in syb2 Het and KO compared with WT; Figure 3, A, C, and E; see direct comparison of groups in Figure 3G). Syb2 is one of the most abundant synaptic proteins, with ~70 copies per synaptic vesicle on average (Takamori *et al.*, 2006) although this number has a high variability among individual vesicles (Mutch *et al.*, 2011). The number of SNAREs proteins per fusion event has been proposed to regulate the kinetics of opening/closure and size of fusion pores (Wu *et al.*, 2017; Bao *et al.*, 2018; Chiang *et al.*, 2018). Thus, the effects of syb2 reduction may be confounded when studying the aggregate retrieval of multiple vesicles, as is the case for our results using high-frequency stimulation. However, when working at the probabilistic limit, as in our experiments monitoring endocytosis of individual synaptic vesicles, the inherent variabilities arising from changes in syb2 copy number in the vesicles become more apparent. While reducing the gene dose of syb2 had no effect on fusion and only a small effect on synaptic vesicle recycling after strong stimulation (Figure 1), syb2 heterozygous synapses showed a significant change in the mode of endocytosis at the single synaptic vesicle level during sparse activity (Figure 3). This effect on endocytosis mode is exacerbated when extracellular Ca^{2+} levels are increased. The Ca^{2+}-dependent slowdown in retrieval is absent in syb2 KO presynaptic terminals; the slower components of endocytosis account for <30% of all endocytosis (in contrast to ~65% in WT and ~55% in Het at 8 mM Ca^{2+}) and most of retrieval is ultrafast (Figure 3, E and F; see direct comparison of groups in Figure 3H). This result resembles the effects on single vesicle endocytosis of deletion of syt1 (Li *et al.*, 2017; Chanaday and Kavalali, 2018). Thus, our results indicate that syb2 and syt1 work together not only in the regulation of Ca^{2+}-dependent fusion of synaptic vesicles, but also in the modulation of the kinetics of retrieval of synaptic vesicle proteins in a Ca^{2+}-dependent manner. Although we cannot exclude that syb2 may interact with other Ca^{2+}-sensing proteins to modulate endocytosis, for example, calmodulin (Quetglas *et al.*, 2000). Even though syb2 and syt1 couple synchronous release to fast (~1–1.5 s) and slow (>3 s) modes of endocytosis in a Ca^{2+}-dependent manner, ultrafast retrieval, detected by optical methods, appears to be relatively independent of Ca^{2+} changes and it remains impervious to elimination of syb2 or syt1, indicating that other mechanisms may underlie this type of recycling. Whether the ultrafast endocytic events described here correspond to a shift toward reversible pore closure due to low amounts of syb2 molecules at the fusion site would require further investigation.

In summary, our new findings suggest a role for syb2, a key component of the canonical SNARE complex, in regulation of synaptic vesicle retrieval at high- and low-frequency levels of evoked activity, which closely follows the previously reported role of its fusion partner, the Ca^{2+} sensor syt1.
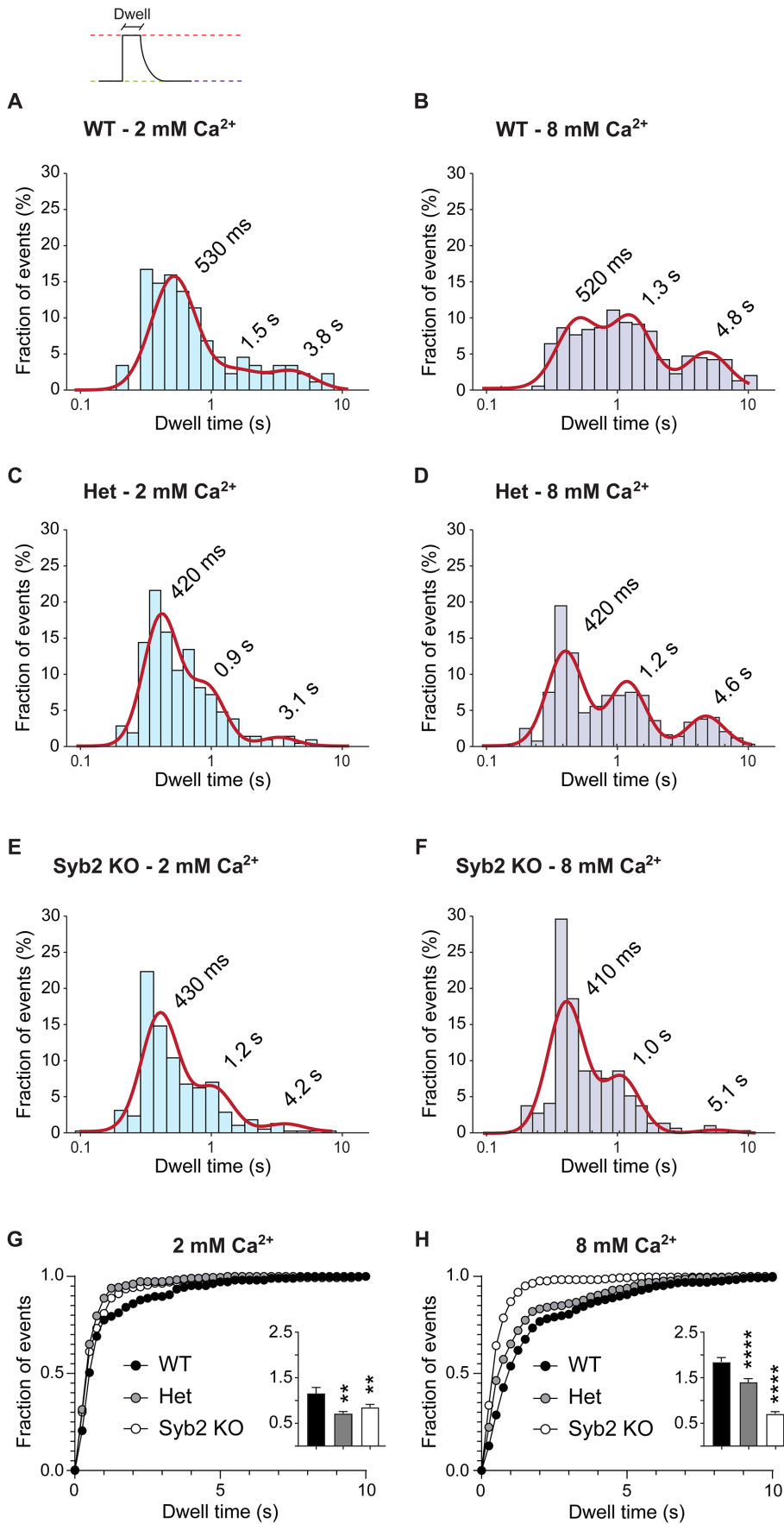
MATERIALS AND METHODS

Dissociated hippocampal cultures

Synaptobrevin-2 KO mice were generated by Thomas C. Südhof laboratory (Schoch *et al.*, 2001). Due to the blethality of syb2 KO, heterozygous mice were crossed and primary hippocampal neuron cultures were performed from E17–19 embryos. This breeding procedure allowed the comparison in each experiment of syb2 KO neurons with littermate WT and heterozygous counterparts. All experiments were performed following protocols approved by the Vanderbilt University Medical Center Institutional Animal Care and Use Committee.

Both hippocampi were dissected in sterile conditions and posteriorly dissociated using 10 mg/ml trypsin and 0.5 mg/ml DNAase for 10 at 37°C. After careful trituration using a P1000 pipette, cells were resuspended to a concentration of 1 pup per six coverslips and plated onto a 12-mm coverslip coated with 1:50 MEM:Matrigel solution. Basic growth medium consisted of MEM medium (no phenol red), 5 g/l d-glucose, 0.2 g/l $NaHCO_3$, 100 mg/l transferrin, 5% of fetal bovine serum, 0.5 mM l-glutamine, 2% B-27 supplement, and 2–4 µM cytosine arabinoside. Cultures were kept in humidified incubators at 37°C and gassed with 95% air and 5% CO_2.

Lentiviral infection

Lentiviruses were produced in HEK293T cells (catalogue no. CRL-1573; ATCC, Manassas, VA) by contransfection of pFUW-vGlut-1pHluorin vector (Li *et al.*, 2017; Chanaday and Kavalali, 2018) and three packaging plasmids (pCMV-VSV-G, pMDLg/pRRE, pRSV-Rev) using Fugene six transfection reagent (catalogue no. E2692; Promega, Madison, WI). The supernatants of the cultures were

FIGURE 3: Deleting syb2 accelerates vGluT1-pHluorin endocytosis after single synaptic fusion. (A–F) Probability distribution of single vesicle dwell times (bars) and Gaussian mix model fit (straight red lines). (G, H) Cumulative distribution of dwell times comparing the different genotypes. Insets: Average dwell time for each experimental group. Kruskall-Wallis test: $p < 0.0001$. Dunn's multiple comparison's test for 2 mM Ca^{2+}: WT vs. Het, $p = 0.0012$; WT vs. syb2 KO, $p = 0.0046$. Dunn's multiple comparison's test for 8 mM Ca^{2+}: WT vs. Het, $p < 0.0001$; WT vs. syb2 KO, $p < 0.0001$. WT 2 mM Ca^{2+} vs. WT 8 mM Ca^{2+}, $p = 0.0002$.

collected 72 h after the transfection and clarified by centrifugation (2000 rpm, 15 min), and subsequently used for infection of DIV 4 hippocampal neurons. All experiments were performed on 18–20 DIV cultures when synapses were mature and lentiviral expression of constructs of interest was optimal.

Live fluorescence imaging

The extracellular solution contained 150 mM NaCl, 4 mM KCl, 10 mM glucose, 10 mM HEPES, 2 mM $MgCl_2$, 2 or 8 mM $CaCl_2$, 10 µM CNQX, and 50 µM AP-5 (to prevent recurrent network activity), with pH 7.4 and 320 mOsM. Fluorescence was recorded using a Nikon Eclipse TE2000-U microscope with a 100× Plan Fluor objective (Nikon, Minato, Tokyo, Japan) attached to an Andor iXon + back-illuminated EMCCD camera (model no. DU-897E-CSO-#BV; Andor Technology, Belfast, UK). For illumination, we used a Lambda-DG4 illumination system (Sutter Instruments, Novato, CA) with a FITC emission filter. Images were acquired at 10 Hz with binning of 4×4 to optimize the signal-to-noise ratio. Neurons were stimulated using parallel bipolar electrodes (FHC, Bowdoin, ME) delivering 35-mA pulses at 20-s intervals, followed by a rest period before the delivery of 200 APs at 40 Hz. Boutons were visualized by the addition of Tyrode's solution with 50 mM NH_4Cl at the end of each experiment. Circular regions of interest of 2.27-µm diameter were automatically drawn around local fluorescence maximums using a custom-made macro for Fiji (Schindelin et al., 2012) and the fluorescent traces obtained were exported to MATLAB (MathWorks, Natick, MA) for analysis using our previously validated automated method (Chanaday and Kavalali, 2018).

Statistical analysis

Histograms of amplitudes and single vesicle dwell time distributions were fitted in MATLAB using a Gaussian mixture model with one to five components and the model with the smallest Bayes information criterion value was automatically selected as the best fit (see Supplemental Table 1). N for each group and experiment are given in the figure legends. Experimental groups were compared using Kruskal-Wallis analysis of medians and Dunn's multiple comparison posttest (test results are given in the figure legends). Bar graphs always give mean values ± SEM.

REFERENCES

Bao H, Das D, Courtney NA, Jiang Y, Briguglio JS, Lou X, Roston D, Cui Q, Chanda B, Chapman ER (2018). Dynamics and number of trans-SNARE complexes determine nascent fusion pore properties. Nature 554, 260–263.

Chanaday NL, Kavalali ET (2018). Optical detection of three modes of endocytosis at hippocampal synapses. eLife 7, e36097.

Chiang CW, Chang CW, Jackson MB (2018). The transmembrane domain of synaptobrevin influences neurotransmitter flux through synaptic fusion pores. J Neurosci 38, 7179–7191.

Deak F, Schoch S, Liu X, Südhof TC, Kavalali ET (2004). Synaptobrevin is essential for fast synaptic-vesicle endocytosis. Nat Cell Biol 6, 1102–1108.

Haberman A, Williamson WR, Epstein D, Wang D, Rina S, Meinertzhagen IA, Hiesinger PR (2012). The synaptic vesicle SNARE neuronal Synaptobrevin promotes endolysosomal degradation and prevents neurodegeneration. J Cell Biol 196, 261–276.

Hosoi N, Holt M, Sakaba T (2009). Calcium dependence of exo- and endocytotic coupling at a glutamatergic synapse. Neuron 63, 216–229.

Imig C, Min SW, Krinner S, Arancillo M, Rosenmund C, Südhof TC, Rhee J, Brose N, Cooper BH (2014). The morphological and molecular nature of synaptic vesicle priming at presynaptic active zones. Neuron 84, 416–431.

Kavalali ET, Jorgensen EM (2014). Visualizing presynaptic function. Nat Neurosci 17, 10–16.

Koo SJ, Kochlamazashvili G, Rost B, Puchkov D, Gimber N, Lehmann M, Tadeus G, Schmoranzer J, Rosenmund C, Haucke V, et al. (2015). Vesicular synaptobrevin/VAMP2 levels guarded by AP180 control efficient neurotransmission. Neuron 88, 330–344.

Leitz J, Kavalali ET (2011). Ca²⁺ influx slows single synaptic vesicle endocytosis. J Neurosci 31, 16318–16326.

Leitz J, Kavalali ET (2016). Ca²⁺ dependence of synaptic vesicle endocytosis. The neuroscientist: a review journal bringing neurobiology, Neurol Psychiatr 22, 464–476.

Li YC, Chanaday NL, Xu W, Kavalali ET (2017). Synaptotagmin-1- and synaptotagmin-7-dependent fusion mechanisms target synaptic vesicles to kinetically distinct endocytic pathways. Neuron 93, 616–631.e613.

Mutch SA, Kensel-Hammes P, Gadd JC, Fujimoto BS, Allen RW, Schiro PG, Lorenz RM, Kuyper CL, Kuo JS, Bajjalieh SM, Chiu DT (2011). Protein quantification at the single vesicle level reveals that a subset of synaptic vesicle proteins are trafficked with high precision. J Neurosci 31, 1461–1470.

Quetglas S, Leveque C, Miquelis R, Sato K, Seagar M (2000). Ca²⁺-dependent regulation of synaptic SNARE complex assembly via a calmodulin- and phospholipid-binding domain of synaptobrevin. Proc Natl Acad Sci USA 97, 9695–9700.

Raingo J, Khvotchev M, Liu P, Darios F, Li YC, Ramirez DM, Adachi M, Lemieux P, Toth K, Davletov B, et al. (2012). VAMP4 directs synaptic vesicles to a pool that selectively maintains asynchronous neurotransmission. Nat Neurosci 15, 738–745.

Schindelin J, Arganda-Carreras I, Frise E, Kaynig V, Longair M, Pietzsch T, Preibisch S, Rueden C, Saalfeld S, Schmid B, et al. (2012). Fiji: an open-source platform for biological-image analysis. Nat Methods 9, 676–682.

Schoch S, Deak F, Konigstorfer A, Mozhayeva M, Sara Y, Südhof TC, Kavalali ET (2001). SNARE function analyzed in synaptobrevin/VAMP knockout mice. Science 294, 1117–1122.

Südhof TC, Rothman JE (2009). Membrane fusion: grappling with SNARE and SM proteins. Science 323, 474–477.

Takamori S, Holt M, Stenius K, Lemke EA, Grønborg M, Riedel D, Urlaub H, Schenck S, Brügger B, Ringler P, et al. (2006). Molecular anatomy of a trafficking organelle. Cell 127, 831–846.

Voglmaier SM, Kam K, Yang H, Fortin DL, Hua Z, Nicoll RA, Edwards RH (2006). Distinct endocytic pathways control the rate and extent of synaptic vesicle protein recycling. Neuron, 51, 71–84.

Wu Z, Thiyagarajan S, O'Shaughnessy B, Karatekin E (2017). Regulation of exocytotic fusion pores by SNARE protein transmembrane domains. Front Mol Neurosci, 10, 315.

Xu J, Luo F, Zhang Z, Xue L, Wu XS, Chiang HC, Shin W, Wu LG (2013). SNARE proteins synaptobrevin, SNAP-25, and syntaxin are involved in rapid and slow endocytosis at synapses. Cell Rep 3, 1414–1421.

Zimmermann J, Trimbuch T, Rosenmund C (2014). Synaptobrevin 1 mediates vesicle priming and evoked release in a subpopulation of hippocampal neurons. J Neurophysiol 112, 1559–1565.